Available online at www.sciencedirect.com

SciVerse ScienceDirect

Ceramics International 38 (2012) 3011–3016

CERAMICS INTERNATIONAL

www.elsevier.com/locate/ceramint

Anti-reduction of Ti^{4+} in $Ba_{4.2}Sm_{9.2}Ti_{18}O_{54}$ ceramics by doping with MgO, Al_2O_3 and MnO_2

Xiaogang Yao *, Huixing Lin, Wei Chen, Lan Luo

Information Materials and Devices Research Center, Shanghai Institute of Ceramics,
Chinese Academy of Science, 1295 Dingxi Road, Shanghai 200050, PR China

Received 14 October 2011; received in revised form 26 November 2011; accepted 29 November 2011
Available online 6 December 2011

Abstract

The anti-reduction of Ti^{4+} ions in $Ba_{4.2}Sm_{9.2}Ti_{18}O_{54}$ (BST) ceramics at high sintering temperature over 1300 °C was investigated. MgO, Al_2O_3 and MnO_2 were added separately to suppress the reduction of Ti^{4+} ions so as to improve the microwave dielectric properties of BST ceramics. The microstructure of BST ceramics was analyzed by X-ray diffraction (XRD) and scanning electron microscopy (SEM). X-ray photoelectron spectroscopy (XPS) was used to study the electroconductivity of BST ceramics and valency changes of Ti ions. The results showed that MgO or Al_2O_3, when acting as an acceptor, could effectively suppress the reduction of Ti^{4+} ions and significantly improve the $Q \times f$ values of BST ceramics at the cost of dielectric constant. Meanwhile, MnO_2 as an oxidant had also improved the $Q \times f$ values but with no decrease in dielectric constant. Excellent microwave dielectric properties were achieved in $Ba_{4.2}Sm_{9.2}Ti_{18}O_{54}$ ceramics doped with 0.2 wt.% Al_2O_3 sintered at 1340 °C for 3 h: $\varepsilon_r = 76.9$, $Q \times f = 10{,}120$ GHz and $\tau_f = -22.7$ ppm/°C.

Keywords: A. Sintering; C. Dielectric properties; D. Perovskite; Ceramics; Crystal structure

1. Introduction

The rapid progress of modern mobile phones and satellite communication systems has created a high demand for the miniaturization of microwave devices. Ceramics with high ε_r, high $Q \times f$ values and near-zero τ_f have been extensively used for miniaturizing the dimensions of the resonators and filters [1].

$Ba_{6-3x}R_{8+2x}Ti_{18}O_{54}$ (R = La, Pr, Nd, Sm) solid solution systems are recognized as an important series of high permittivity microwave dielectric ceramics with dielectric constant ranging from 80 to 130 [2,3]. $Ba_{6-3x}Sm_{8+2x}Ti_{18}O_{54}$ system, as a member in this family, exhibits $\varepsilon_r \approx 80$, $Q \times f \approx 8000$ GHz and $\tau_f \approx -8$ ppm/°C at $x = 0.6$ [4]. Researches on this solid solution are commonly focused on these aspects: (a) control the τ_f value to near zero [5–7]; (b) substitution of A or B site in tungsten bronze structure [8–10]; (c) low temperature sintering [11–13]. Nevertheless, little attention has been attached to the improvement on $Q \times f$ values, which is of vital importance to microwave devices.

As reported by Templeton and Pullar [14,15], titanium dioxide ceramics tend to deoxidize at high temperature above 1300 °C or with deficient oxygen supply during sintering. The deoxidized reaction undergoes as below:

$$TiO_2 \rightarrow TiO_{2-x} + x/2O_2\uparrow \qquad (1)$$

Oxygen vacancies appear and tend to catch electrons to form *F*-color centers. A dark hole appears in central part of the sample when these electrons are emitted by combining with Ti^{4+} ions near-by to form $[Ti^{4+}e^-]$, which drastically increases the dielectric loss of TiO_2 ceramics. Similar dark holes have also been found in BST ceramics, with an undesirable impact on microwave dielectric properties. Templeton and Wang [14] reported that improved $Q \times f$ values were attained by adding a divalent or trivalent acceptor ion that has approximately equal radius to that of Ti^{4+} into TiO_2 ceramic. Whether this is also true for BST ceramics or not still needs to be demonstrated. Doping with a transition metal oxide, functioning as an oxidant, such as MnO_2 for instance [15], can also prevent the

---

* Corresponding author. Tel.: +86 21 5241 4112; fax: +86 21 5241 3903.
E-mail address: rockyao@student.sic.ac.cn (X. Yao).

0272-8842/$36.00 © 2011 Elsevier Ltd and Techna Group S.r.l. All rights reserved.
doi:10.1016/j.ceramint.2011.11.082

reduction of Ti^{4+} as shown below:

$$Mn^{4+} + Ti^{3+} \rightarrow Mn^{3+} + Ti^{4+} \tag{2}$$

$$Mn^{3+} + Ti^{3++} \rightarrow Mn^{2+} + Ti^{4+} \tag{3}$$

In the present study, MgO, Al_2O_3, MnO_2 are added to $Ba_{4.2}Sm_{9.2}Ti_{18}O_{54}$ ceramics and the mechanism of anti-reduction of Ti^{4+} by acceptor-doping has been investigated.

2. Experimental procedure

$Ba_{4.2}Sm_{9.2}Ti_{18}O_{54}$ ceramics were prepared by conventional solid-state reaction method. The raw materials—$BaCO_3$ (99.9%), Sm_2O_3 (99.9%), and TiO_2 (99.9%) powders were weighed according to the desired stoichiometry of $Ba_{4.2}Sm_{9.2}Ti_{18}O_{54}$. The powders were ground in deionized water for 24 h with ZrO_2 balls. The mixture was dried at 120 °C, and then calcined at 1150 °C in air for 3 h [16]. The calcined powders were mixed with 0.2 wt.% MgO (99.9%), Al_2O_3 (99.9%) and MnO_2 (99.5%) separately. Afterwards the mixtures were milled for 24 h, dried at 120 °C and granulated with polyvinyl alcohol (PVA). The granules were preformed and then sintered at 1300–1380 °C in air for 3 h with a heating rate of 5 °C/min.

The crystalline phase was identified using a Rigaku D/max 2550V X-ray diffractometer with a conventional Cu-Kα radiation in the range of 10–70° with a step size of 0.02°. The microstructure of BST ceramics was examined by a Hitachi S-4800 field emission scanning electron microscope. An ESCAlab250 X-ray photoelectron spectroscopy was used to observe the variation of electroconductivity and valency in center and edge of sintered BST samples. The method developed by Hakki and Coleman [17] was used to measure the microwave dielectric properties of the polished pellets. The measurement frequencies range from 3 to 4 GHz. All the microwave measurements were used in the TE_{011} mode of an Agilent E8363A PNA series network analyzer. τ_f was tested in the temperature range from 20 to 80 °C and can be calculated by noting the change in resonant frequency as:

$$\tau_f = \frac{f_2 - f_1}{60 f_1} \tag{4}$$

Here, f_1 and f_2 represent the resonant frequencies at 20 and 80 °C, respectively.

3. Results and discussion

3.1. Crystalline phase

Fig. 1a shows the X-ray diffraction patterns of $Ba_{4.2}Sm_{9.2}Ti_{18}O_{54}$ ceramics doped with none, MgO, Al_2O_3 and MnO_2 sintered at 1340 °C for 3 h. Only a single $BaSm_2Ti_4O_{12}$ phase is identified for a small amount of addition. However, it is found in Fig. 1b that diffraction peaks of BST ceramics doped with Al_2O_3 shift slightly toward higher 2θ degree values, while those doped with MgO or MnO_2 are exactly the opposite. It can be deduced, according to Bragg's law, that doping with Al_2O_3 has decreased the lattice parameters, but MgO or MnO_2 have expanded the lattice structure. The lattice parameters and volumes of BST ceramics shown in Table 1 are in accordance with what we deduced. We can infer from Table 2 that the lattice structure contracts only if the substitution of Ti^{4+} by Al^{3+} happens.

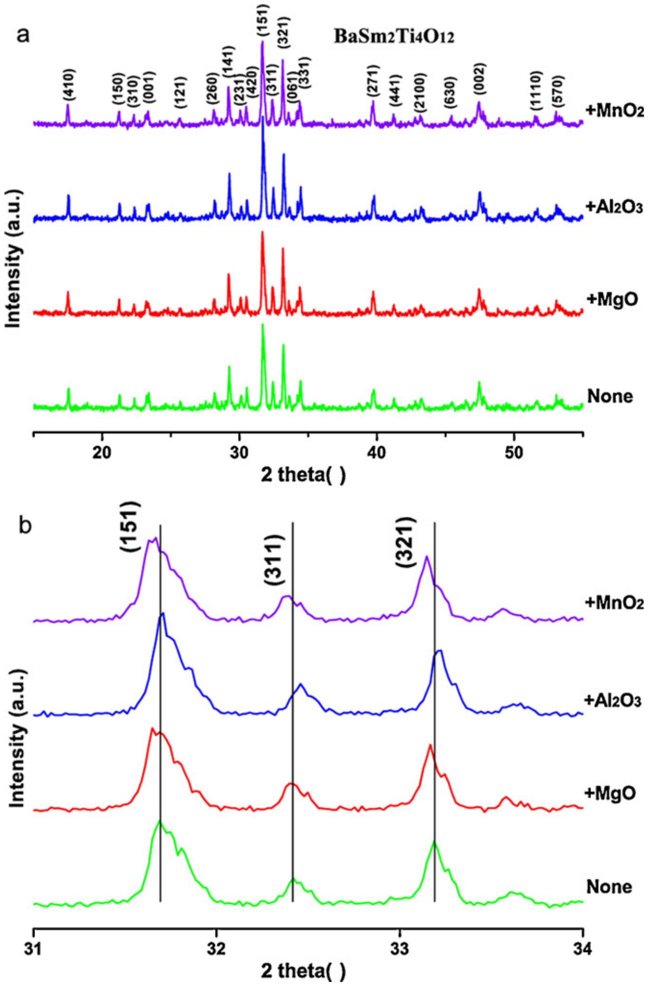

Fig. 1. Whole (a) and partial (b) X-ray diffraction patterns of $Ba_{4.2}Sm_{9.2}Ti_{18}O_{54}$ ceramics doped with none, MgO, Al_2O_3 and MnO_2 sintered at 1340 °C for 3 h.

3.2. Density

Fig. 2 shows the density of $Ba_{4.2}Sm_{9.2}Ti_{18}O_{54}$ ceramics doped with none, MgO, Al_2O_3 and MnO_2 sintered at different temperatures for 3 h. The density of undoped BST ceramics increases with the increasing of the sintering temperature, and

Table 1
Lattice parameters of $Ba_{4.2}Sm_{9.2}Ti_{18}O_{54}$ ceramics doped with none, MgO, Al_2O_3 and MnO_2.

Sample	a/Å	b/Å	c/Å	V/$Å^3$
Undoped	22.295	22.322	22.280	22.317
+MgO	12.139	12.148	12.138	12.163
+Al_2O_3	3.828	3.830	3.826	3.832
+MnO_2	1036.10	1038.52	1034.62	1040.22

Table 2
Ionic radius and polarizability [18,19].

Ion	Radius (Å)	Polarizability (Å^3)
Mg^{2+}	0.72	1.33
Al^{3+}	0.54	0.78
Mn^{2+}	0.91	2.64
Ba^{2+}	1.35	6.40
Sm^{3+}	0.96	4.74
Ti^{4+}	0.60	2.94

then remains unchanged. BST ceramics doped with MnO_2 shows the same regularity and almost equal values with undoped ones. Doping with MgO or Al_2O_3 has slightly decreased the density of BST ceramics.

3.3. Microstructure

To investigate the changes in densification and grain size of the samples, the natural surfaces of the sintered specimens were examined. SEM images of BST ceramics with different additives are shown in Fig. 3. All show single typical columnar grain morphology that usually observed in $Ba_{6-3x}R_{8+2x}Ti_{18}O_{54}$ (R = La, Nd, Sm) ceramics. The SEM results confirm the single phase of $BaSm_2Ti_4O_{12}$ identified by X-ray diffraction above. Adding MgO made the grains grow bigger and more homogeneous, while smaller and more compact grains were formed in BST ceramics doped with Al_2O_3. Sample with MnO_2 shows evidence of discontinuous grain growth, with some much larger grains having developed amongst other much smaller grains, resulting in a less homogenous microstructure.

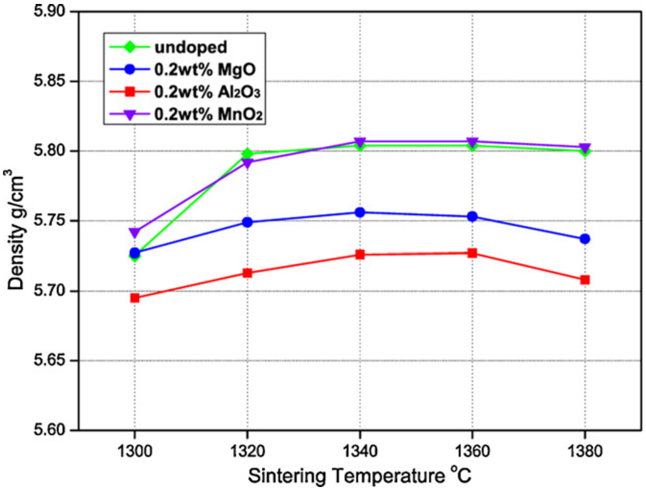

Fig. 2. Density of $Ba_{4.2}Sm_{9.2}Ti_{18}O_{54}$ ceramics doped with none, MgO, Al_2O_3 and MnO_2 sintered at different temperatures for 3 h.

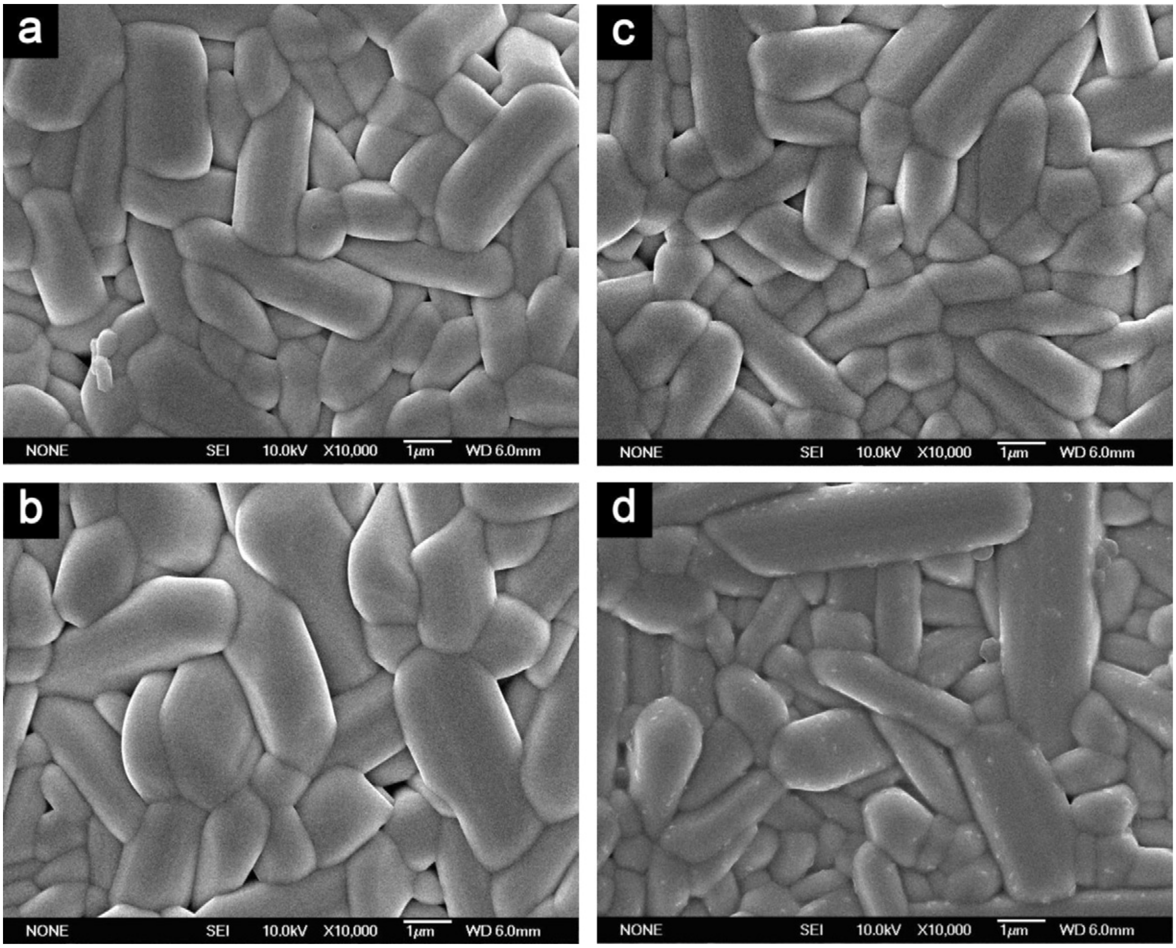

Fig. 3. SEM micrographs of $Ba_{4.2}Sm_{9.2}Ti_{18}O_{54}$ ceramics doped with: (a) none, (b) MgO, (c) Al_2O_3, (d) MnO_2 sintered at 1340 °C for 3 h.

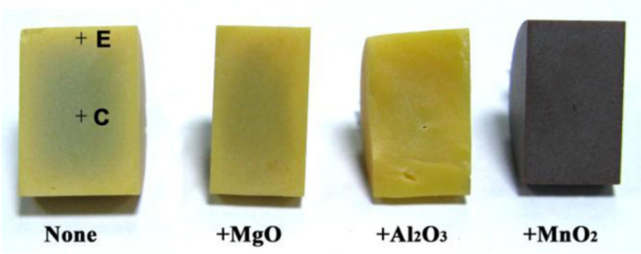

Fig. 4. Cross sections of $Ba_{4.2}Sm_{9.2}Ti_{18}O_{54}$ ceramics doped with: none, MgO, Al_2O_3 and MnO_2.

3.4. Dark hole

Fig. 4 shows the cross sections of BST ceramics doped with: none, MgO, Al_2O_3 and MnO_2. A large dark area is observed in undoped BST ceramic. As mentioned above, it has a direct relation to the absorption of light when electrons generated in the deoxidation process are emitted. The increase of electroconductivity brought about by electron transfer in the internal structure has a very bad influence on the dielectric properties. Nevertheless, the dark area is much smaller in BST ceramic doped with MgO, and disappears in the one with Al_2O_3, similar to the results reported by Pullar and Penn for doped TiO_2 [15]. No useful evidence is obtained from the BST ceramic doped with MnO_2, as it undergoes a thorough change in color to black. It is revealed that acceptor dopants are effective to cure the "dark hole".

3.5. Valency analysis

Fig. 5 shows the results of XPS analysis on the center and edge of the cross sections of BST ceramics doped with none, Al_2O_3 and MnO_2. Five characteristic photoelectronic spectra: O1s, Ti2p1, Ti2p3, Ti3s and Ti3p are measured to show the distinction of electroconductivity. As shown in Fig. 5, undoped BST ceramic has an obvious shift of all the spectra, with an average shift of 2.15 eV. A denser charge distribution indicated in the center than at the edge. However, this difference is minimized effectively with a small amount of Al_2O_3 or MnO_2 added.

XPS data of the three BST specimens are listed in Table 3. An obvious change in FWHM is found in the Ti3s and Ti3p spectra of the undoped BST ceramic. The enlargement of FWHM in the center of the sample is closely related to the presence of Ti^{3+}, whose photoelectron spectrum is very near to, or overlaps with, that of Ti^{4+}. However, little difference in FWHM of all the spectra is observed in BST ceramics doped with Al_2O_3 or MnO_2. From the above, the conclusion is reached that adding an acceptor or oxidant has positive effect on the anti-reduction of Ti^{4+} in BST ceramics.

3.6. Anti-reduction mechanism

Taking MgO for example, in an acceptor-doping system, the reaction below occurs with increasing of temperature:

$$MgO \xrightarrow{TiO_2} Mg''_{Ti} + V_o^{\bullet\bullet} + O_o \qquad (5)$$

The other two reactions happen during sintering as below:

$$O_o^{\times} \leftrightarrow 1/2O_2 + V_o^{\bullet\bullet} + 2e \qquad (6)$$

$$Ti^{4+} + e \leftrightarrow Ti^{3+} \qquad (7)$$

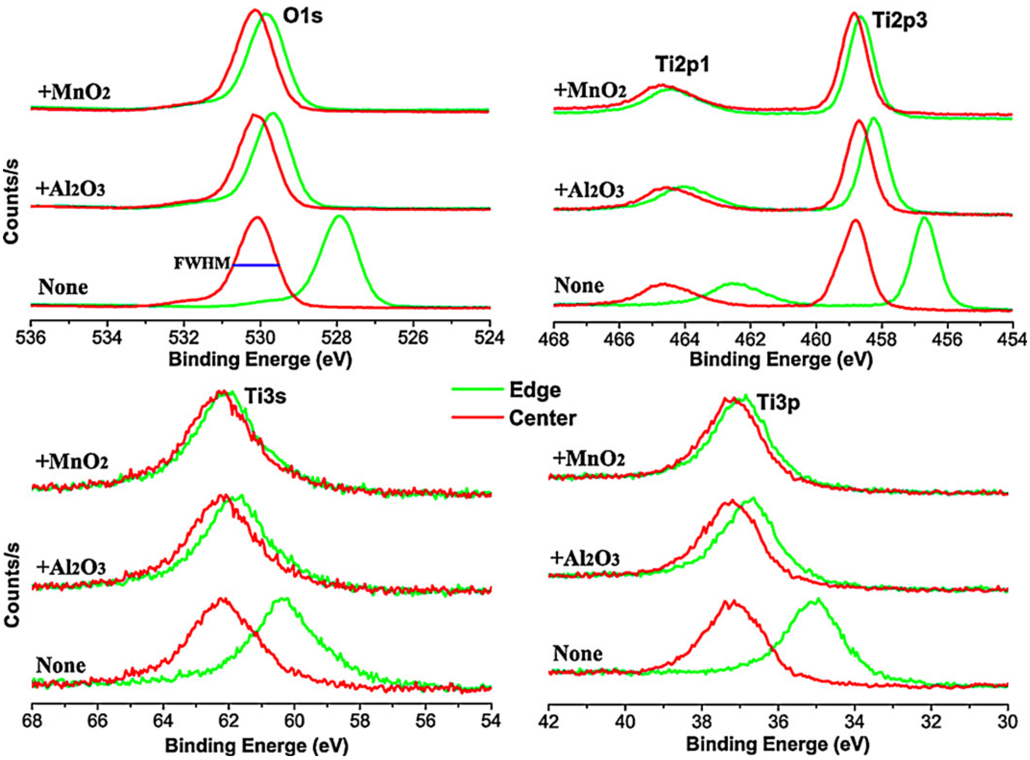

Fig. 5. XPS graphs of the center and edge of the cross sections of $Ba_{4.2}Sm_{9.2}Ti_{18}O_{54}$ ceramics doped with none, Al_2O_3 and MnO_2.

Table 3
XPS data of BST ceramics doped with none, Al_2O_3 and MnO_2.

Sample	Photoelectron spectrum	BE peak[a] (eV)		ΔBE (eV)	FWHM[b] (eV)	
		C	E		C	E
BST	O1s	530.10	527.95	2.15	1.14	1.14
	Ti2p1	464.65	462.55	2.10	1.87	1.84
	Ti2p3	458.80	456.70	2.10	0.92	0.91
	Ti3s	62.25	60.10	2.15	2.26	2.05
	Ti3p	37.15	34.95	2.20	1.77	1.58
BST + Al_2O_3	O1s	530.20	529.65	0.55	1.14	1.14
	Ti2p1	464.55	464.10	0.45	1.85	1.85
	Ti2p3	458.80	458.25	0.55	0.91	0.91
	Ti3s	62.10	61.60	0.50	2.03	2.01
	Ti3p	37.20	36.65	0.55	1.55	1.53
BST + MnO_2	O1s	530.15	529.90	0.25	1.15	1.14
	Ti2p1	464.70	464.50	0.20	1.86	1.85
	Ti2p3	458.85	458.65	0.20	2.07	2.04
	Ti3s	62.15	61.90	0.25	0.93	0.94
	Ti3p	37.15	36.85	0.30	1.58	1.56

[a] BE = binding energy.
[b] FWHM = full length of half maximum.

It is easy to understand that acceptor-doping reaction (5) produces a certain amount of oxygen vacancies ($V_o^{\bullet\bullet}$) in the process of heating. These oxygen vacancies would suppress the deoxidizing reaction (6) to produce fewer electrons, which would further suppress the reduction of Ti^{4+} in reaction (7).

3.7. Dielectric properties

Fig. 6 shows the dielectric constant of $Ba_{4.2}Sm_{9.2}Ti_{18}O_{54}$ ceramics doped with none, MgO, Al_2O_3 and MnO_2 sintered at different temperatures for 3 h. The relationship between dielectric constant and sintering temperature reveals the same trend as that between density and sintering temperature since a higher density means a lower porosity. Thus, the BST ceramics doped with MnO_2 has the highest dielectric constant, while the ones with Al_2O_3 lowest. On the other hand, the dielectric constant is directly affected by the polarizabilities of filling ions. As shown in Table 2, substitution of high polarizability Ti^{4+} ($\alpha = 2.94$ Å^3) ion by much lower Mg^{2+} ($\alpha = 1.33$ Å^3) or Al^{3+} ($\alpha = 0.78$ Å^3) ion leads to a decrease of total polarizability, thus decreases the whole dielectric constant distinctly.

Fig. 7 shows the $Q \times f$ values of $Ba_{4.2}Sm_{9.2}Ti_{18}O_{54}$ ceramics doped with none, MgO, Al_2O_3 and MnO_2 sintered at different temperatures for 3 h. Undoped BST ceramics have the lowest $Q \times f$ values with a maximum of 8090 GHz at 1340 °C. However, BST ceramics doped with Al_2O_3 show the highest $Q \times f$ values with a maximum of 10,120 GHz. The $Q \times f$ values of the ceramics with MgO or MnO_2 are lower, but still better than for the undoped ceramic. It is

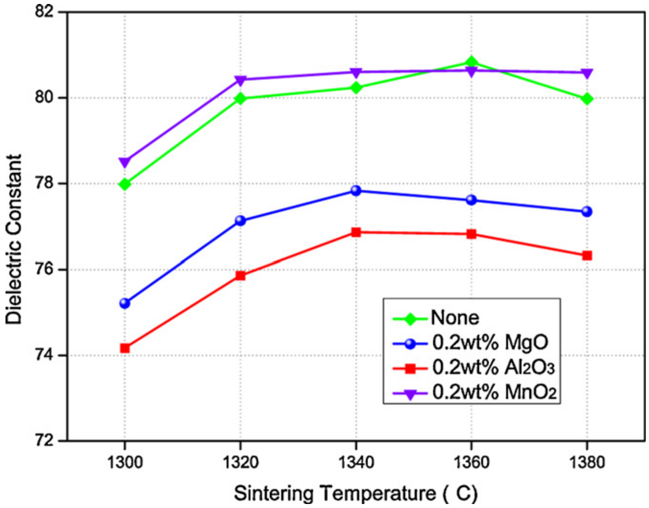

Fig. 6. Dielectric constant of $Ba_{4.2}Sm_{9.2}Ti_{18}O_{54}$ ceramics doped with none, MgO, Al_2O_3 and MnO_2 sintered at different temperatures for 3 h.

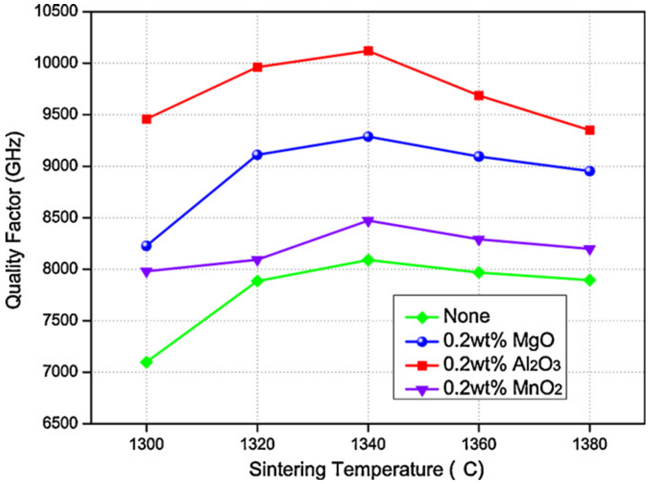

Fig. 7. $Q \times f$ values of $Ba_{4.2}Sm_{9.2}Ti_{18}O_{54}$ ceramics doped with none, MgO, Al_2O_3 and MnO_2 sintered at different temperatures for 3 h.

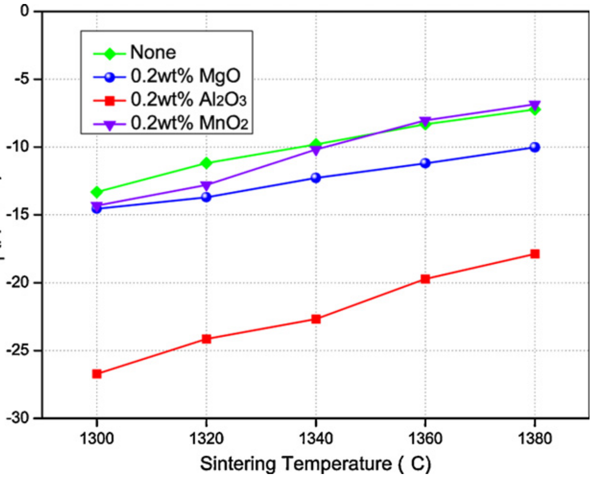

Fig. 8. τ_f values of $Ba_{4.2}Sm_{9.2}Ti_{18}O_{54}$ ceramics doped with none, MgO, Al_2O_3 and MnO_2 sintered at different temperatures for 3 h.

revealed that both acceptor doping and oxidant doping are beneficial for the $Q \times f$ values of BST ceramics, as they prevent the reduction of Ti^{4+}.

Fig. 8 shows the τ_f values of $Ba_{4.2}Sm_{9.2}Ti_{18}O_{54}$ ceramics doped with none, MgO, Al_2O_3 and MnO_2 sintered at different temperatures for 3 h. Raising sintering temperature from 1300 °C to 1380 °C leads to a gradual increase of τ_f. Adding MgO or MnO_2 has little influence on τ_f. However, the τ_f values of BST ceramics doped with Al_2O_3 are more negative than undoped ones, increasing from −26.7 to −17.8 ppm/°C.

4. Conclusions

Three metallic oxides were employed as either acceptor (MgO, Al_2O_3) or oxidant (MnO_2) to study the anti-reduction of Ti^{4+} in $Ba_{4.2}Sm_{9.2}Ti_{18}O_{54}$ ceramics at high sintering temperature. Both acceptor doping and oxidant doping play an important roll in the anti-reduction of Ti^{4+} in BST ceramics. BST ceramics doped with MgO or Al_2O_3 have significant improvement on $Q \times f$ values, but non-ignorable decrease in dielectric constant. BST ceramics doped with MnO_2 have improved $Q \times f$ values and almost unchanged dielectric constant. Adding MgO or MnO_2 has tiny effect on τ_f values while doping Al_2O_3 make τ_f values much more negative.

References

[1] I.M. Reaney, D. Iddles, Microwave dielectric ceramics for resonators and filters in mobile phone networks, J. Am. Ceram. Soc. 89 (2000) 2063–2072.

[2] H. Ohsato, M. Mizuta, T. Okuda, Microwave dielectric properties of tungsten bronze type $Ba_{6-3x}R_{8+2x}Ti_{18}O_{54}$ (R = La, Pr, Nd, and Sm) solid solutions, J. Ceram. Soc. Jpn. 106 (1998) 178–182.

[3] S.Y. Wu, Y. Li, X.M. Chen, Raman spectra of $Ba_{6-3x}Sm_{8+2x}Ti_{18}O_{54}$ solid solution, J. Phys. Chem. Solids 64 (2003) 2365–2368.

[4] H. Ohsato, Science of tungsten bronze type like $Ba_{6-3x}R_{8+2x}Ti_{18}O_{54}$ (R = rare earth) microwave dielectric solid solution, J. Eur. Ceram. Soc. 21 (2001) 2703–2711.

[5] S.F. Wang, Y.F. Hsu, Densification, microstructural evolution and dielectric properties of $Ba_{6-3x}(Sm_{1-y}Nd_y)_{8+2x}Ti_{18}O_{54}$, J. Eur. Ceram. Soc. 26 (2006) 1629–1635.

[6] H. Ohsato, A. Komura, Microwave dielectric properties and sintering of $Ba_{6-3x}R_{8+2x}Ti_{18}O_{54}$ (R = Sm, x = 2/3) solid solution with added rutile, J. Appl. Phys. 37 (1998) 5357–5359.

[7] J.H. Zhu, W.Z. Lu, Effects of $SrTiO_3$ additives on the structure and microwave dielectric properties of $Ba_{4.2}Sm_{9.2}Ti_{18}O_{54}$ ceramics, Ceram. Int. 35 (2009) 855–860.

[8] I. Kagomiya, M. Suzuki, Microwave dielectric properties of tungsten-bronze type like $(Ba_{1-a}Sr_a)_{6-3x}R_{8+2x}Ti_{18}O_{54}$(R = Sm, Nd) solid solutions, J. Eur. Ceram. Soc. 27 (2007) 3059–3062.

[9] N. Qin, X.M. Chen, Effects of Sm/Bi co-substitution on microstructures and microwave dielectric characteristics of $Ba_{6-3x}La_{8+2x}Ti_{18}O_{54}$, Mater. Sci. Eng. B 111 (2004) 90–94.

[10] S.Y. Wu, Y. Li, X.M. Chen, Raman spectra of Nd/Sn co-substituted $Ba_{6-3x}Sm_{8+2x}Ti_{18}O_{54}$ microwave dielectric ceramics, J. Appl. Phys. 96 (2004) 5683–5686.

[11] J.M. Yoon, J.A. Lee, Sintering behavior and microwave dielectric characteristics of $BaO–Sm_2O_3–4TiO_2$ ceramics with B_2O_3 and BaB_2O_4, J. Eur. Ceram. Soc. 26 (2006) 2129–2133.

[12] C.C. Cheng, T.E. Hsieh, Effects of composition on low temperature sinterable Ba–Nd–Sm–Ti–O microwave dielectric materials, J. Eur. Ceram. Soc. 24 (2004) 1787–1790.

[13] L.E. Chang, B.S. Chiou, W.H. Lee, Effect of glass additions on the sintering behavior and electrical microwave properties of $BaO–Nd_2O_3–Sm_2O_3–TiO_2$ ceramics, J. Mater. Sci. Mater. Electron. 15 (2004) 153–158.

[14] A. Templeton, X.R. Wang, Microwave dielectric loss of titanium oxide, J. Am. Ceram. Soc. 83 (2000) 95–100.

[15] R.C. Pullar, S.J. Penn, Dielectric loss caused by oxygen vacancies in titanium ceramics, J. Eur. Ceram. Soc. 29 (2009) 419–424.

[16] H.X. Lin, L. Luo, Sintering and microwave dielectric properties of $La(Mg_{0.5}Ti_{0.5})O_3$ ceramics doped with $La_2O_3–BaO_3–TiO_2$ glass, J. Appl. Phys. 47 (2008) 7243–7245.

[17] B.W. Hakki, P.D. Coleman, A dielectric resonator method of measuring inductive capacitance in the millimeter range, IRE Trans. Microw. Theory Tech. (1960) 402–410.

[18] M.T. Sebastian, Dielectric Materials for Wireless Communication, 2008, pp. 531–539..

[19] R.D. Shannon, Dielectric polarizabilities of ions in oxides and fluorides, J. Appl. Phys. 73 (1993) 348–366.